

~~CONFIDENTIAL~~

CLASSIFICATION CHANGED

UNCLASSIFIED

NACA

Authority of *NASA* *Documentation* *1017*  
*and* *May 20, 1975* *H4-7-1-65*

# RESEARCH MEMORANDUM

for the

Bureau of Aeronautics, Department of the Navy

OF

REFERENCE

EFFECTS OF VARIOUS MODIFICATIONS ON

THE STATIC LONGITUDINAL STABILITY AND CONTROL

CHARACTERISTICS OF A 0.065-SCALE MODEL OF THE

DO NOT REMOVE FROM THE ROOM

CHANCE VOUGHT REGULUS II MISSILE

AT A MACH NUMBER OF 2.01

TRD NO. NACA AD 398

By Ross B. Robinson and Cornelius Driver

Langley Aeronautical Laboratory  
Langley Field, Va.

CLASSIFIED DOCUMENT

This document contains classified information affecting the National Defense of the United States within the meaning of the Espionage Act, USC 18793 and 791. Its transmission or the revelation of its contents in any manner to an unauthorized person is prohibited by law.

## NATIONAL ADVISORY COMMITTEE FOR AERONAUTICS

WASHINGTON

~~CONFIDENTIAL~~

UNCLASSIFIED



## NATIONAL ADVISORY COMMITTEE FOR AERONAUTICS

## RESEARCH MEMORANDUM

for the

Bureau of Aeronautics, Department of the Navy

EFFECTS OF VARIOUS MODIFICATIONS ON  
THE STATIC LONGITUDINAL STABILITY AND CONTROL  
CHARACTERISTICS OF A 0.065-SCALE MODEL OF THE  
CHANCE VOUGHT REGULUS II MISSILE  
AT A MACH NUMBER OF 2.01

TED NO. NACA AD 398

By Ross B. Robinson and Cornelius Driver

## SUMMARY

An investigation has been conducted in the Langley 4- by 4-foot supersonic pressure tunnel to determine the effects on the static longitudinal stability and control characteristics of various modifications to a 0.065-scale model of the Chance Vought Regulus II missile. The modifications consisted of a control housing on top of the fuselage, two sizes of canard surfaces with fixed incidence angles, various angles of nose droop, and two types of inlet boundary-layer bleed diverters. The tests were made at a Mach number of 2.01 and a Reynolds number, based on the mean aerodynamic chord of  $1.54 \times 10^6$ .

## INTRODUCTION

One of the most significant results of a previous investigation of the Regulus II missile at Mach numbers of 1.41 to 2.01 (ref. 1) was the large negative value of pitching-moment coefficient at zero lift ( $C_{m_0}$ ) for zero control deflection. A free-flight rocket model test (unpublished) showed the same result, the value of the negative  $C_{m_0}$  obtained being somewhat larger than that for the tunnel model. The occurrence of these

~~CONFIDENTIAL~~  
UNCLASSIFIED

large values of  $C_{m_0}$  necessitates large control deflections for trim with a resultant increase in drag and loss of maneuverability.

The results presented in reference 1 indicate that the negative increments of  $C_{m_0}$  might be attributable, in part, to effects of the underslung scoop-type inlet. In addition, static loadings of the free-flight model produced moderate deflections of a long section of the nose. Since both the free-flight model and a production missile would be more flexible than the wind-tunnel model, additional negative increments in  $C_{m_0}$  might be expected.

Means of reducing this initial negative  $C_{m_0}$  are of considerable importance. The basic tunnel model previously tested was modified to provide experimental information on the use of canard surfaces to produce a positive increment in  $C_{m_0}$  for zero control deflection and on the effects of nose droop on the longitudinal characteristics. Other modifications to the configuration included an external control housing on top of the fuselage and means for varying the amount of flow through the boundary-layer bleed of the scoop-type inlet.

This report presents the results of an investigation of the effects of these modifications on the aerodynamic characteristics in pitch of the Regulus II missile at  $M = 2.01$  in the Langley 4- by 4-foot supersonic pressure tunnel.

#### COEFFICIENTS AND SYMBOLS

The results of the tests are presented as standard NACA coefficients of forces and moments. The data are referred to the stability-axes system (fig. 1) with the reference center of moments on the longitudinal center line of the basic body of revolution at a longitudinal station corresponding to the leading edge of the wing mean geometric chord (fig. 2).

The coefficients and symbols are defined as follows:

|           |   |
|-----------|---|
| $C_L$     | lift coefficient, $-Z/qS$                   |
| $C_D$     | drag coefficient, $Drag/qS$                 |
| $C_m$     | pitching-moment coefficient, $M'/qS\bar{c}$ |
| $C_{m_0}$ | pitching-moment coefficient at $C_L = 0$    |
| X         | force along X-axis                          |

|                   |  |
|-------------------|--|
| Z                 | force along Z-axis   |
| M'                | moment about Y-axis  |
| q                 | free-stream dynamic pressure                                 |
| M                 | Mach number  |
| S                 | wing area including body intercept, 88.47 sq in.             |
| S <sub>c</sub>    | exposed area of canard surface                               |
| $\frac{S_c}{S_w}$ | ratio of exposed area of canard to total wing area           |
| b                 | wing span, 15.63 in.   |
| c                 | chord, in.   |
| $\bar{c}$         | wing mean geometric chord, 5.78 in.                          |
| $\alpha$          | angle of attack of fuselage center line, deg                 |
| t                 | airfoil thickness, in.                                       |
| x                 | chordwise distance from leading edge of airfoil section, in. |
| $\delta_c$        | canard deflection with respect to fuselage center line, deg  |
| $\delta_e$        | elevon deflection normal to hinge line, deg                  |
| L/D               | lift-drag ratio, $C_L/C_D$                                   |
| $m/m_0$           | mass-flow ratio  |
| Subscripts:       |  |
| trim              | measured for $C_m = 0$                                       |
| R                 | right  |
| L                 | left   |

## MODEL AND APPARATUS

A three-view drawing of the basic model and details of various components are presented in figures 2 and 3. Details of the various modifications are shown in figure 4. The geometric characteristics of the model are presented in table I.

The model was equipped with a wing having  $43.5^\circ$  of sweep of the quarter-chord line, aspect ratio 2.75, taper ratio 0.6, and modified circular-arc airfoil sections of 4-percent thickness-chord ratio. (See table I.) The wing was mounted 0.26 inch above the fuselage center line and had zero incidence and dihedral.

Elevons of the plain trailing-edge-flap type provided both longitudinal and lateral control (fig. 2). The model had a swept vertical tail and movable rudder (fig. 2). Deflections of all control surfaces were set manually. The rudder deflection was  $0^\circ$  for the entire test.

Coordinates of the basic fuselage are presented in table II. A simulated static pressure probe was attached to the nose of the fuselage. A scoop inlet equipped with a boundary-layer diverter (fig. 3) was incorporated into the fuselage to simulate the internal flow conditions of the missile. The inlet airflow, which could be throttled manually to provide variable mass-flow ratios, was discharged out the rear of the fuselage around the sting. A solid fairing (fig. 3) was used to permit investigations of the model with no internal airflow ("inlet faired closed" configuration).

Modifications to the basic model (fig. 4) consisted of: (a) a control housing on the top of the fuselage; (b) two fixed-incidence horizontal canard surfaces, the larger having a  $9.5^\circ$  incidence angle, the smaller having a  $19.1^\circ$  incidence angle; (c) various wedges to provide nose-droop angles of  $0^\circ$ ,  $-1.65^\circ$ , and  $-3.00^\circ$ ; and (d) inlet boundary-layer bleed diverters to provide 40-percent and 100-percent closure of the original bleed. When the boundary-layer bleed was completely closed, the bleed outlet under the wing was also sealed.

Force and moment measurements were made through the use of an experimental, all welded, six-component strain-gage balance furnished by the NACA. This experimental balance is characterized by an extremely small size but has an attendant increase in balance deflections and interactions. Space limitation was the primary consideration in its selection.

The following pressure measurements were made:

- (1) the static pressure in the balance chamber inside the model,
- (2) the static pressure on the rim base area of the fuselage, and
- (3) the

total and static pressures of the exit airflow with open inlet by means of a total head rake fastened to the sting at the base of the model.

TEST CONDITIONS AND PROCEDURE

The conditions for the tests were:

|   |                    |
|---|--------------------|
| Mach number . . . . .                                     | 2.01               |
| Reynolds number, based on $\bar{c}$ . . . . .             | $1.54 \times 10^6$ |
| Stagnation pressure, lb/sq in. . . . .                    | 13                 |
| Stagnation temperature, $^{\circ}\text{F}$ . . . . .      | 100                |
| Stagnation dewpoint, $^{\circ}\text{F}$ . . . . .         | < -25              |
| Mach number variation . . . . .                           | $\pm 0.015$        |
| Flow angle in horizontal or vertical plane, deg . . . . . | $\pm 0.1$          |

Tests were made through an angle-of-attack range from about  $-4^{\circ}$  to about  $+12^{\circ}$  at zero angle of sideslip.

CORRECTIONS AND ACCURACY

The angles of attack and sideslip were corrected for the deflection of the balance and sting under load. The nominal values for elevon deflection presented in this report are not corrected for deflection due to load. Although the variation of rudder deflection was not known, it was assumed to be small (within  $\pm 0.1^{\circ}$ ) since the surface was rigidly fixed in the desired position by a bead of solder along the leading edge of the rudder.

Base pressure measurements were made and the longitudinal-force coefficients of all configurations were adjusted to free-stream static pressure at the base. For all configurations with the open inlet, the internal pressure in the model balance chamber was measured and corrections for a buoyant force on the balance were applied to the results. The internal drag was determined from the change in momentum from free-stream conditions to measured conditions at the duct exit. Base drag, buoyant force, and internal drag have been subtracted from the total longitudinal-force measurements so that a net external longitudinal-force coefficient was obtained. The mass-flow ratio was 0.93. The magnitude of the base, internal, and buoyant drag coefficients at  $\alpha = 0^{\circ}$  is indicated by the following table:

|                          |         |
|--------------------------|---------|
| Base $C_D$ . . . . .     | -0.0001 |
| Internal $C_D$ . . . . . | 0.0050  |
| Buoyant $C_D$ . . . . .  | -0.0125 |

The estimated errors in the individual measured quantities are as follows:

|   |             |
|---|-------------|
| $C_L$ . . . . .   | $\pm 0.003$ |
| $C_D$ . . . . .   | $\pm 0.002$ |
| $C_m$ . . . . .   | $\pm 0.005$ |
| $\alpha$ , deg . . . . .  | $\pm 0.1$   |
| $\delta_e$ (corrected for deflection of elevon under load), deg . . . | $\pm 0.1$   |
| $M$ . . . . .   | $\pm 0.015$ |

## RESULTS AND DISCUSSION

### Effects of Nose Droop

Negative deflection of the nose produced a progressive negative shift of pitching-moment coefficient (fig. 5). It is possible that nose bending contributed to the more negative  $C_{m_0}$  experienced by the free-flight rocket model (unpublished results). The results of the present wind-tunnel tests indicate that a nose droop of about  $2^\circ$  would be required to produce the free-flight  $C_{m_0}$  value.

It might be expected that positive deflection of the nose could profitably be used to produce a positive  $C_{m_0}$  shift and thereby reduce the control deflection required for trim.

There was no appreciable effect of nose droop on the static stability and no effect on the lift or drag except above  $C_L \approx 0.3$  where nose droop caused a decrease in  $C_{L\alpha}$  and increased  $C_D$  for constant  $C_L$ .

### Effects of Canards

Addition of either the large or small canards essentially eliminated the large negative value of  $C_{m_0}$  (fig. 6); consequently, the elevon deflections required for trim would be reduced. The large positive increment of  $C_m$  provided by the larger canard at higher values of  $C_L$  probably results from a greater portion of the body nose being affected by the carry-over lift from the canard. The more linear lift and pitching-moment coefficient variation above  $C_L \approx 0.4$  for the configurations having the canards may result from downwash from the canards reducing the effective angle of attack of the inboard portion of the wing.

The effects of elevon deflection on the aerodynamic characteristics in pitch for the model with the large canard are shown in figure 7. The effects of the large canard on the longitudinal characteristics for  $\alpha = 0^\circ$  and for trim ( $C_m = 0^\circ$ ) are presented in figures 8 and 9, respectively. Results for the basic configuration were obtained from reference 1. At  $\alpha = 0^\circ$  the canard produced a slight decrease in total lift coefficient and a positive increment in pitching-moment coefficient, which largely eliminated the negative value of  $C_{m_0}$  of the basic configuration (fig. 8). As a result, about  $10^\circ$  less elevon deflection is required to trim the model at zero lift (fig. 9). In addition, the maximum value of  $C_{L_{trim}}$  obtainable with an elevon deflection of  $-20^\circ$  is increased and the trim drag coefficient is reduced considerably so that higher trim lift-drag ratios are indicated.

#### Effects of Closure of Inlet Boundary-Layer Bleed

The effects on the longitudinal characteristics of closing the boundary-layer bleed of the open-inlet configuration for zero elevon deflection ( $\delta_e = 0$ ) are shown in figure 10. Reducing the bleed air flow 40 percent had only negligible effects, but completely closing the bleed produced a slightly higher lift-curve slope and a positive shift of the pitching-moment curve, reducing the negative value of  $C_{m_0}$  to half that obtained for the open bleed. Similar effects were obtained for  $\delta_e = 20^\circ$  with the 100-percent closed bleed (fig. 11). The elevon effectiveness was about the same for the open and fully closed bleed (fig. 11).

Large longitudinal effects were found when the complete inlet was faired closed. The more linear lift curve and the large positive increment in  $C_m$  for the faired-closed inlet configuration probably result from the altered pressure distribution on the underside of the wing and the aft portion of the fuselage. Fairing the inlet in this manner produces the effect of a cambered surface with a resulting down load behind the center of moments.

#### Effects of Control Housing

The addition of the control housing had little effect on the longitudinal characteristics except for a slight negative shift of the pitching-moment curve (fig. 12).

[REDACTED]

## CONCLUSIONS

The results of an investigation of the effects of various modifications to a 0.065-scale model of the Chance Vought Regulus II missile indicate the following conclusions:

1. Negative deflection of the nose produces a progressive negative shift of the pitching-moment curves. It appears possible that nose bending contributed to the more negative value of pitching-moment coefficient for zero lift ( $C_{m_0}$ ) experienced by a free-flight rocket model.

2. The addition of a fixed-incidence horizontal canard surface resulted in a positive shift in  $C_{m_0}$  and a large increase in the trim lift coefficient and the trim lift-drag ratio obtainable.

3. Complete closure of the inlet boundary-layer air bleed resulted in a positive increment of pitching-moment coefficient throughout the lift-coefficient range.

4. Addition of the control housing had negligible effect on the longitudinal characteristics.

Langley Aeronautical Laboratory,  
National Advisory Committee for Aeronautics,  
Langley Field, Va., August 31, 1955.

*Ross B. Robinson*

Ross B. Robinson  
Aeronautical Research Scientist

*Cornelius Driver*

Cornelius Driver  
Aeronautical Research Scientist

Approved:

*John V. Becker*

John V. Becker

Chief of Compressibility Research Division

mjg

## REFERENCE

1. Robinson, Ross B., Driver, Cornelius, and Spearman, M. Leroy: Static Longitudinal and Lateral Stability and Control Characteristics of an 0.065-Scale Model of the Chance Vought Regulus II Missile at Mach Numbers of 1.41, 1.61, and 2.01 - TED NO. NACA AD 398. NACA RM SL55E31, Bur. Aero., 1955.
- [REDACTED]

TABLE I

## GEOMETRIC CHARACTERISTICS OF MODEL

## Wing:

|  |       |
|--|-------|
| Total area, including fuselage intercept, sq in. . . . . | 88.47 |
| Span, in. . . . .  | 15.63 |
| Root chord, in. . . . .                                  | 7.08  |
| Tip chord, in. . . . .                                   | 4.27  |
| Length of mean geometric chord, $\bar{c}$ , in. . . . .  | 5.78  |
| Aspect ratio . . . . .                                   | 2.75  |
| Taper ratio . . . . .                                    | 0.60  |
| Sweep angle of $\bar{c}/4$ line, deg . . . . .           | 43.5  |
| Airfoil section, streamwise -                            |       |
| Maximum thickness, percent chord . . . . .               | 4.0   |
| Location of maximum thickness, percent chord . . . . .   | 53.7  |
| Trailing-edge thickness, percent chord . . . . .         | 0.04  |
| Symmetric airfoil section defined by                     |       |
| $t/c = 0.122496 - 0.015168x/c - (0.028768(x/c)^2 -$      |       |
| $0.033096(x/c) + 0.0150052)^{1/2}$                       |       |
| Dihedral, deg . . . . .                                  | 0     |
| Incidence, deg . . . . .                                 | 0     |

## Elevons:

|  |      |
|--|------|
| Area behind hinge line, each, sq in. . . . .     | 4.61 |
| Moment of area, each, in. <sup>3</sup> . . . . . | 2.49 |
| Span, in. . . . .                                | 3.43 |
| Sweep of hinge line, deg . . . . .               | 37.3 |

## Vertical Tail:

|  |              |
|--|--------------|
| Span (to model center line), in. . . . .         | 5.07         |
| Area (to model center line), sq in. . . . .      | 23.08        |
| Tip chord (theoretical), in. . . . .             | 2.35         |
| Root chord, in. . . . .                          | 7.16         |
| Length of tail mean geometric chord, in. . . . . | 5.28         |
| Aspect ratio . . . . .                           | 1.12         |
| Taper ratio (theoretical tip) . . . . .          | 0.33         |
| Rudder area, sq in. . . . .                      | 2.35         |
| Airfoil section . . . . .                        | Same as wing |

TABLE I.- Concluded

## GEOMETRIC CHARACTERISTICS OF MODEL

## Fuselage:

|   |       |
|---|-------|
| Length (without probe), in. . . . .                     | 44.15 |
| Maximum diameter, in. . . . .                           | 3.25  |
| Maximum cross-sectional area, sq in. . . . .            | 11.10 |
| Base inner diameter, in. . . . .                        | 2.01  |
| Sting diameter, in. . . . .                             | 1.25  |
| Area of rim of base, sq in. . . . .                     | 0.45  |
| Annular area at base for internal flow, sq in. . . . .  | 1.94  |
| Maximum length-diameter ratio . . . . .                 | 13.6  |
| Total base area (annular + rim + sting), sq in. . . . . | 3.62  |

## Canards:

## Small -

|                                   |        |
|-----------------------------------|--------|
| Area (exposed), sq in. . . . .    | 0.64   |
| Span (body included), in. . . . . | 1.65   |
| Deflection angle, deg . . . . .   | 19.1   |
| $\frac{S_c}{S_w}$ . . . . .       | 0.0072 |

## Large -

|                                   |        |
|-----------------------------------|--------|
| Area (exposed), sq in. . . . .    | 1.28   |
| Span (body included), in. . . . . | 2.17   |
| Deflection angle, deg . . . . .   | 9.5    |
| $\frac{S_c}{S_w}$ . . . . .       | 0.0144 |

## Dorsal Fairing:

|                             |      |
|-----------------------------|------|
| Length, in. . . . .         | 31.0 |
| Width, maximum, in. . . . . | 1.4  |

TABLE II

## COORDINATES OF THE BASE FUSELAGE

[x is distance from nose in inches;  
r is radius in inches]

| x      | r     |
|--------|-------|
| 0.000  | 0.000 |
| .038   | .018  |
| .075   | .033  |
| .150   | .061  |
| .225   | .085  |
| .300   | .107  |
| .450   | .148  |
| .601   | .184  |
| .751   | .218  |
| .901   | .250  |
| 1.502  | .362  |
| 2.252  | .486  |
| 3.003  | .596  |
| 3.754  | .698  |
| 4.505  | .792  |
| 6.006  | .964  |
| 7.508  | 1.117 |
| 9.009  | 1.255 |
| 10.511 | 1.376 |
| 12.012 | 1.478 |
| 13.514 | 1.567 |
| 15.015 | 1.625 |
| 34.761 | 1.625 |
| 37.765 | 1.586 |
| 40.086 | 1.493 |
| 41.850 | 1.345 |
| 42.850 | 1.245 |
| 43.850 | 1.115 |
| 44.150 | 1.065 |

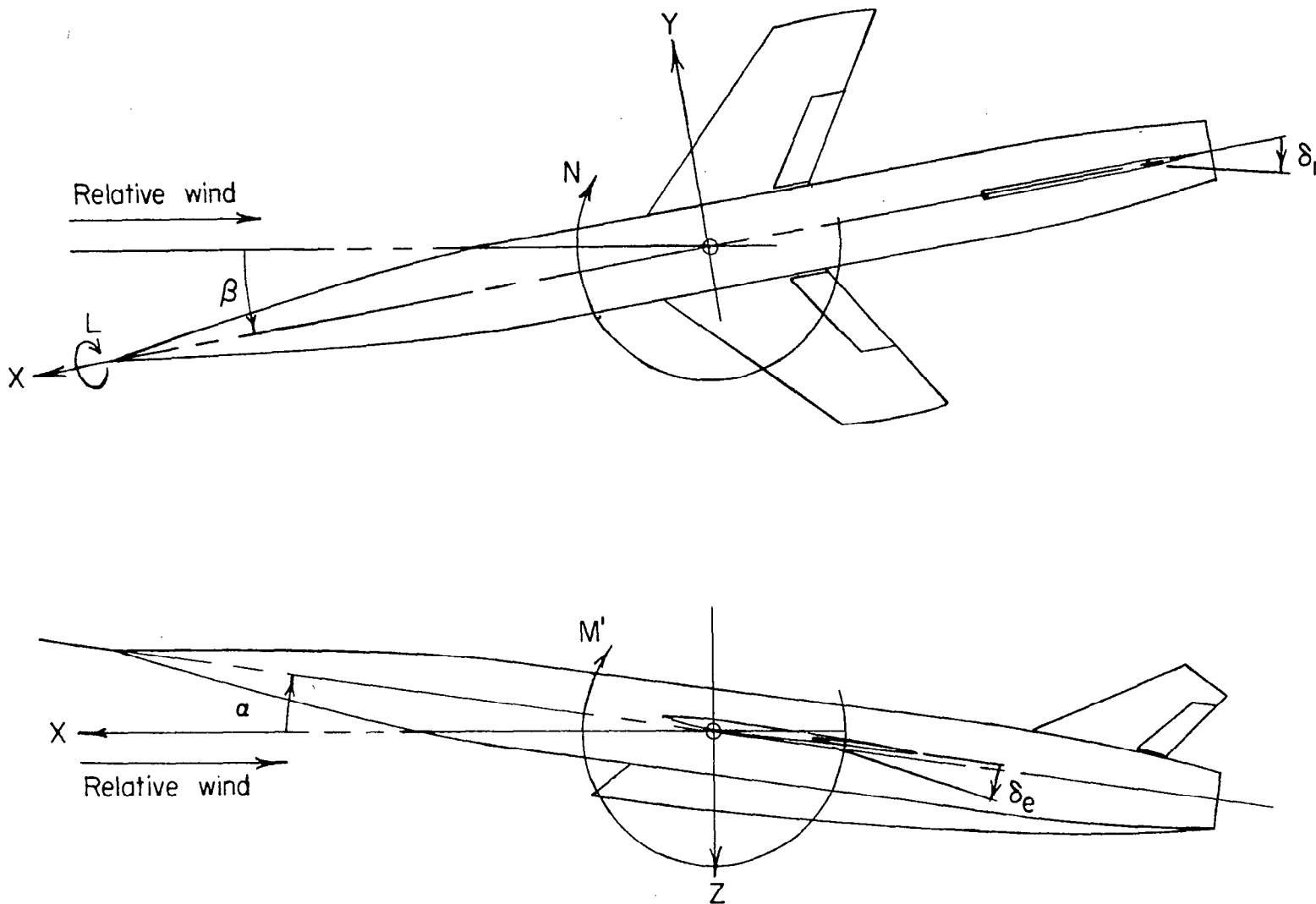
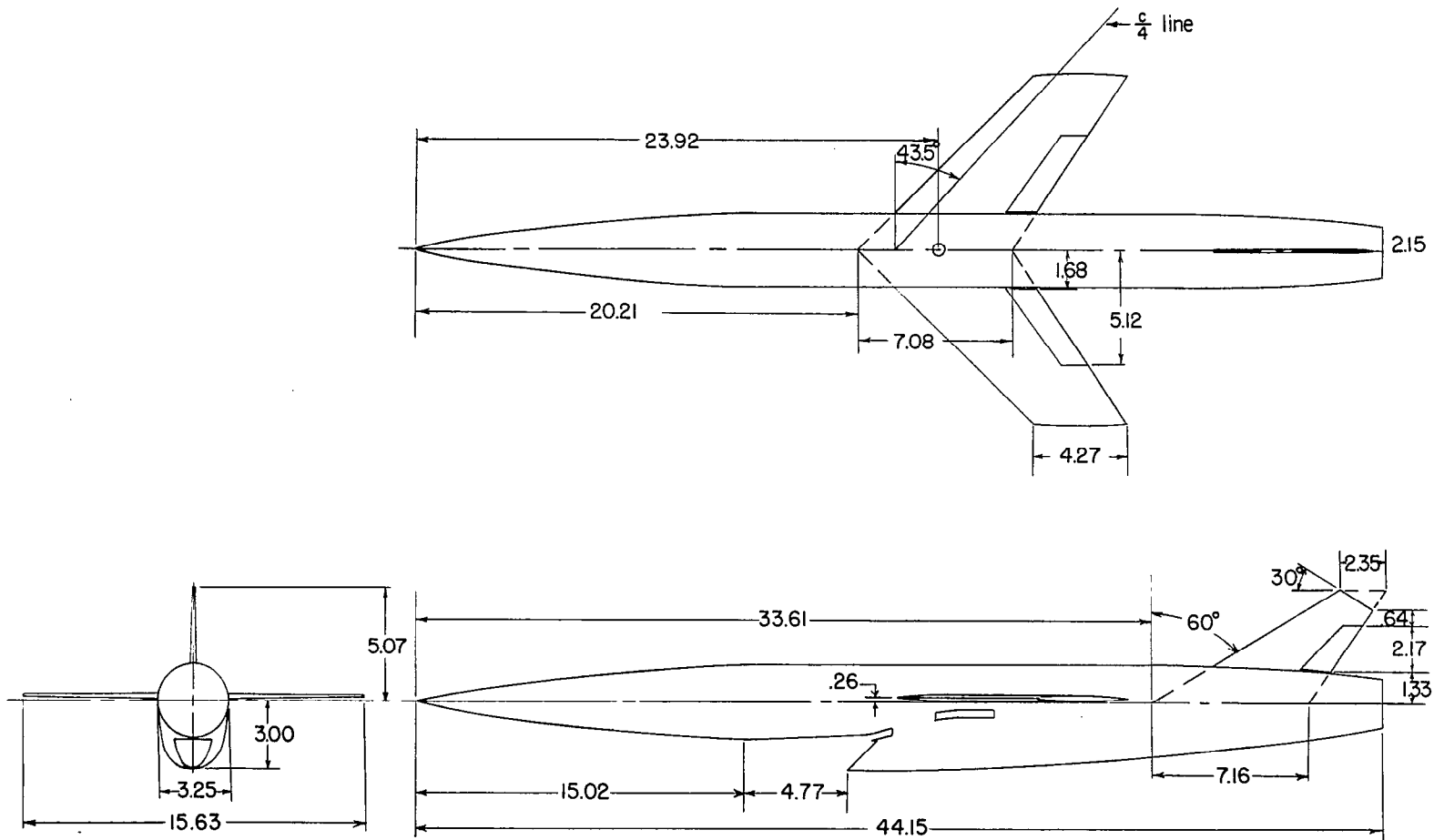
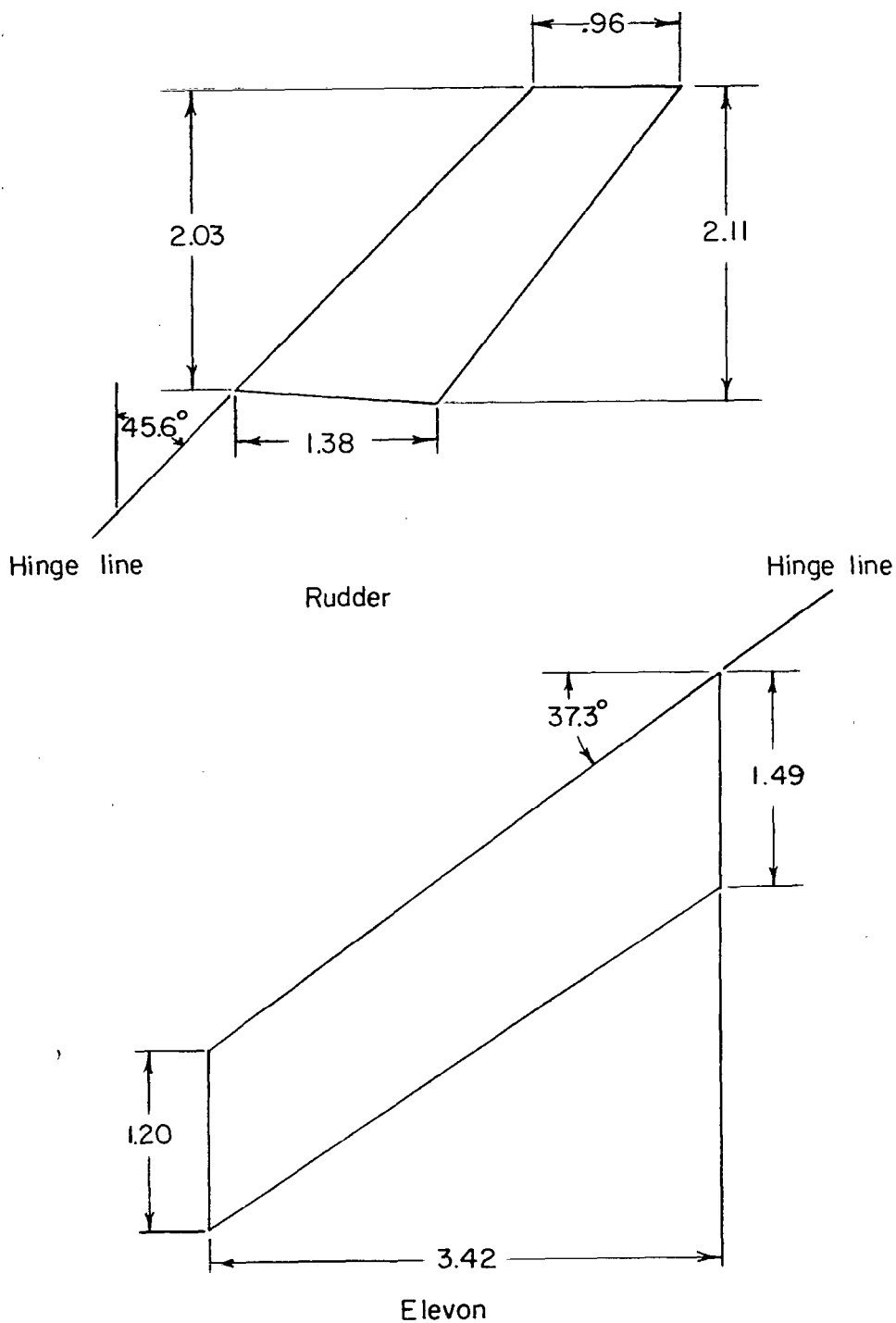


Figure 1.- System of stability axes. Arrows indicate positive values.



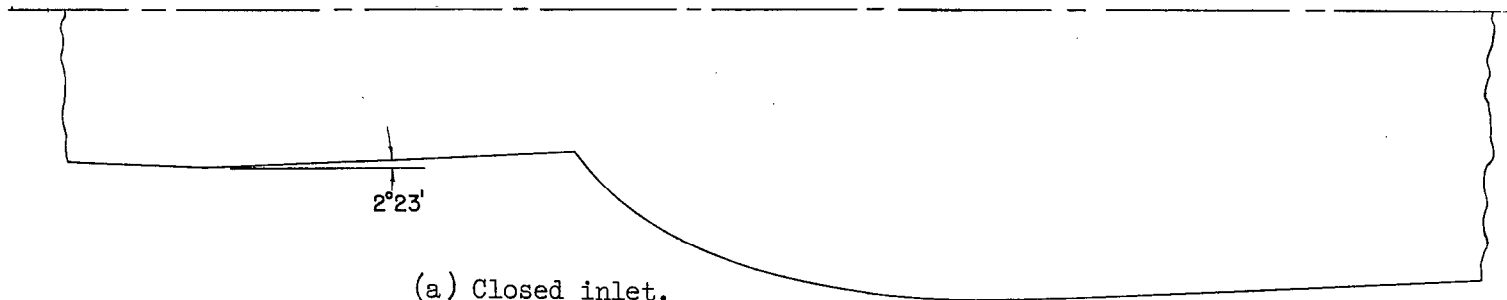
(a) Three-view drawing of model.

Figure 2.- Details of model.



(b) Details of rudder and elevon.

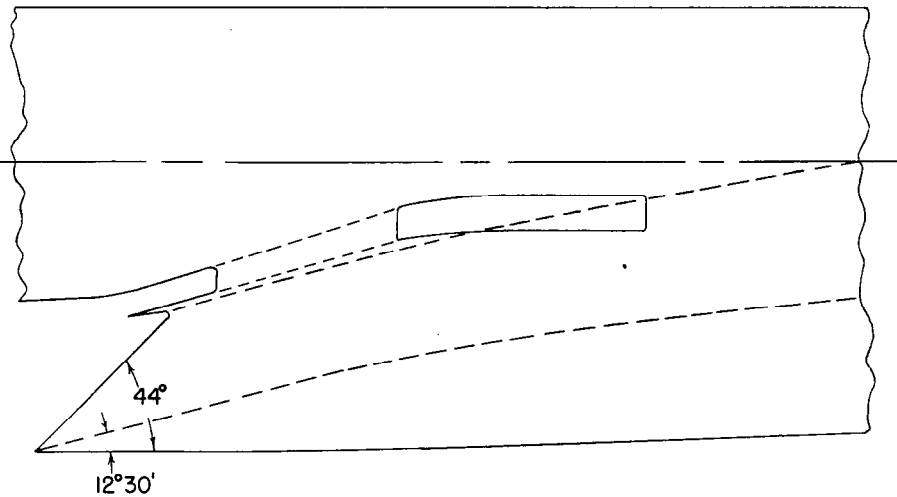
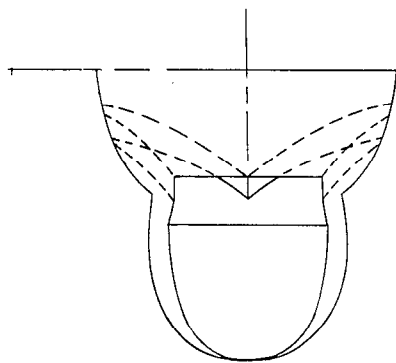
Figure 2.- Concluded.



(a) Closed inlet.

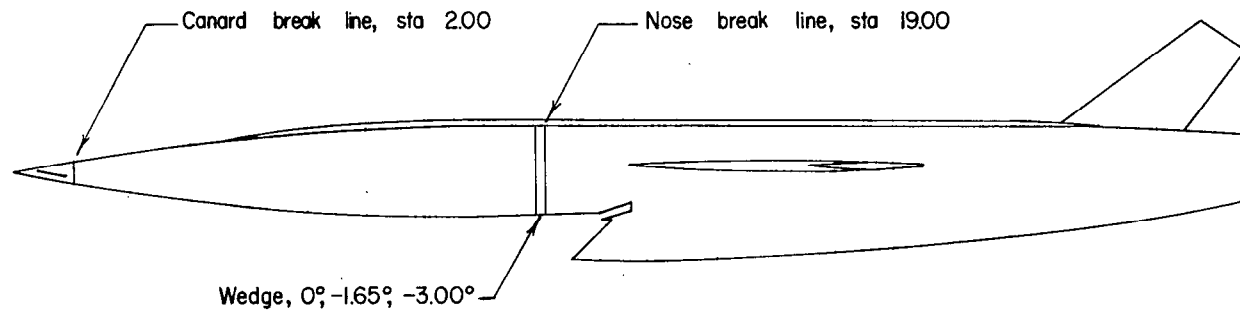
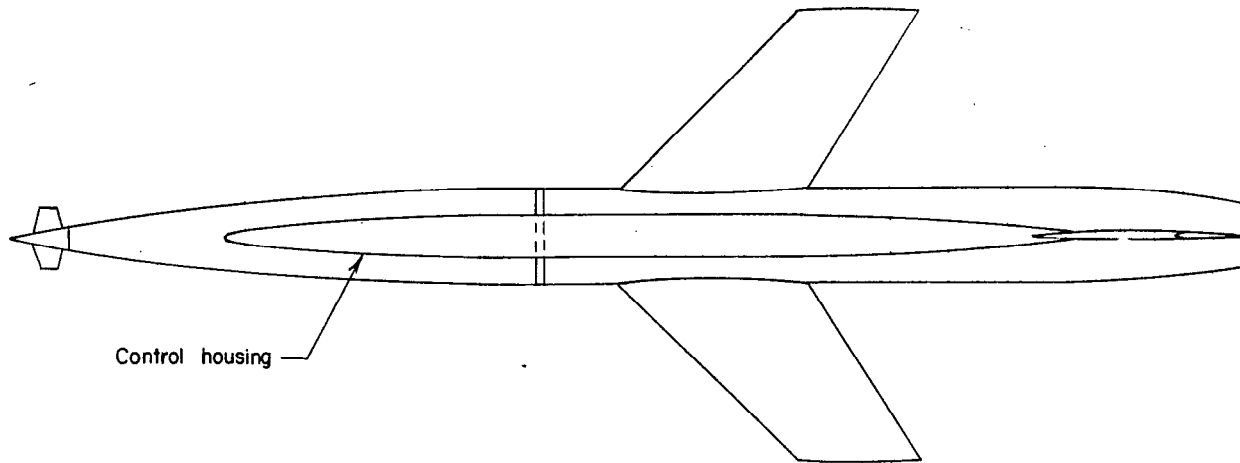
Areas:

|                                     |                    |
|-------------------------------------|--------------------|
| Capture (Normal to center line)     | 206 square inches  |
| Boundary-layer bleed, inlet         | 0.37 square inches |
| Boundary-layer bleed, outlet (each) | 1.08 square inches |



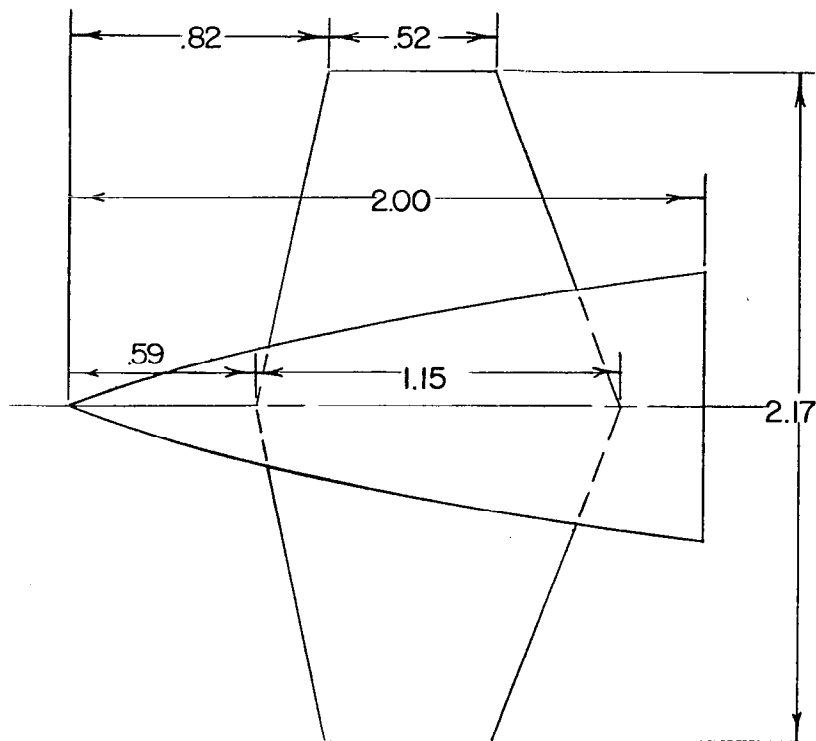
(b) Open inlet.

Figure 3.- Inlet details, open and faired closed.

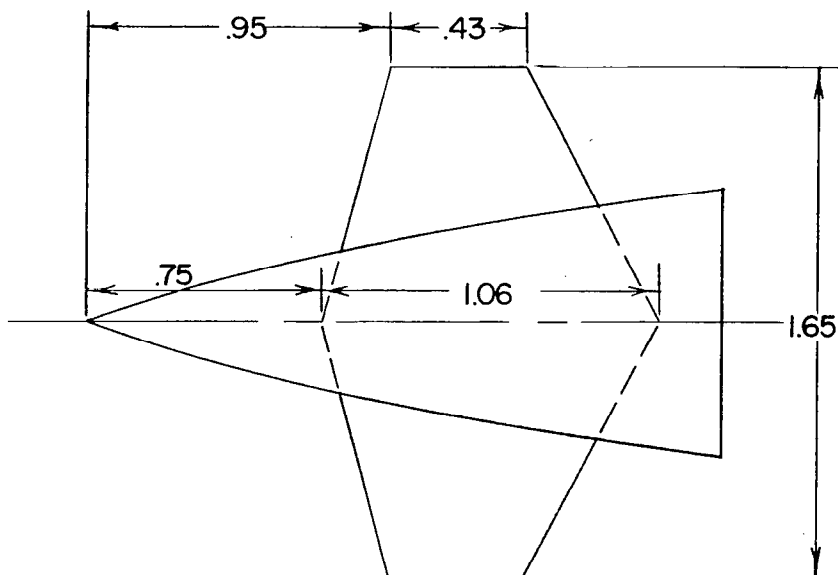


(a) Canard, control housing, and nose wedge.

Figure 4.- Sketches of modifications tested. All dimensions in inches unless otherwise noted. Station 0 is at nose.



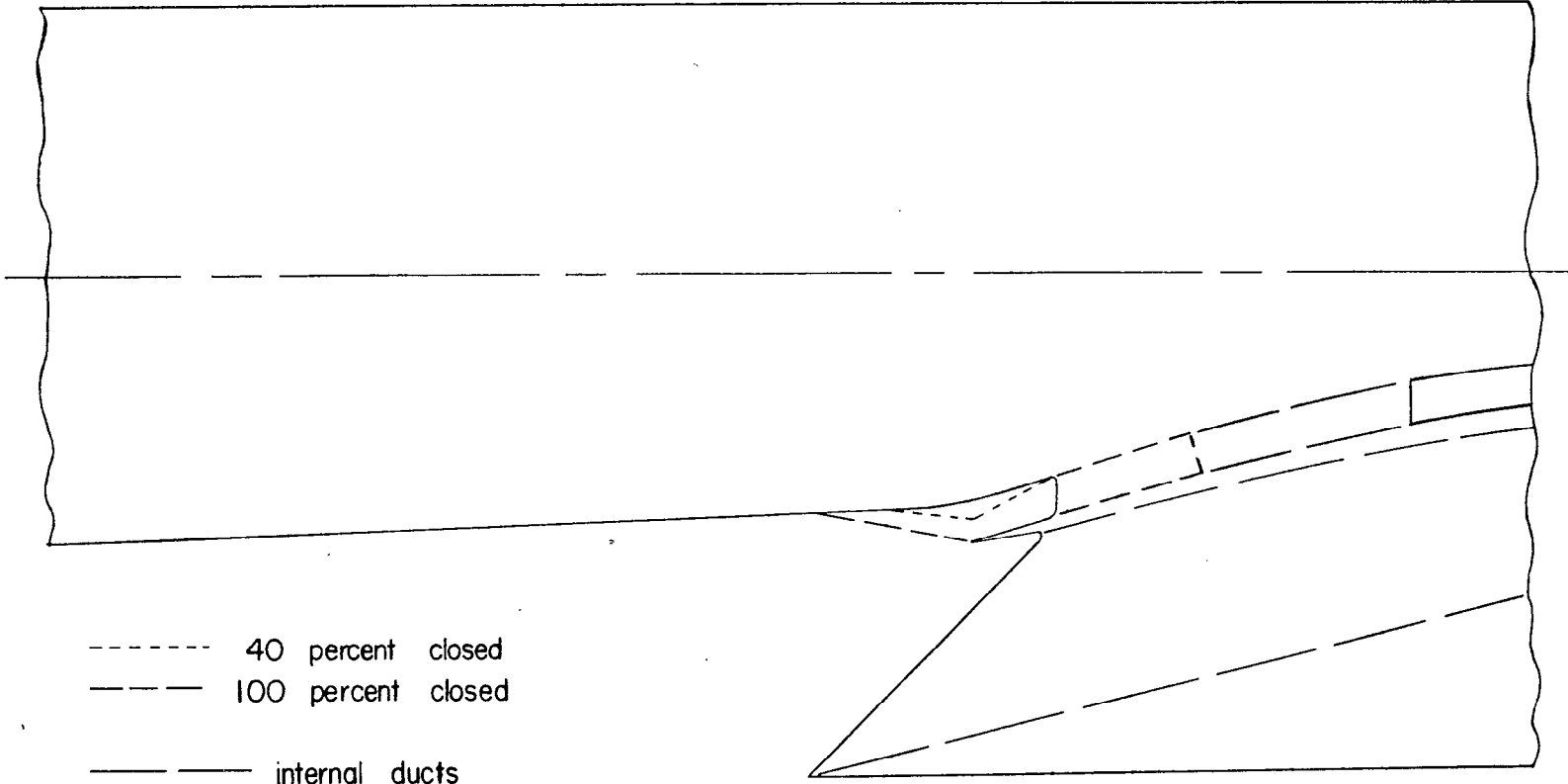
$\delta = 9.5^\circ$ ; exposed area = 1.28 sq in.



$\delta = 19.1^\circ$ ; exposed area = 0.64 sq in.

(b) Details of canards.

Figure 4.- Continued.



(c) Boundary-layer bleed closures.

Figure 4.- Concluded.

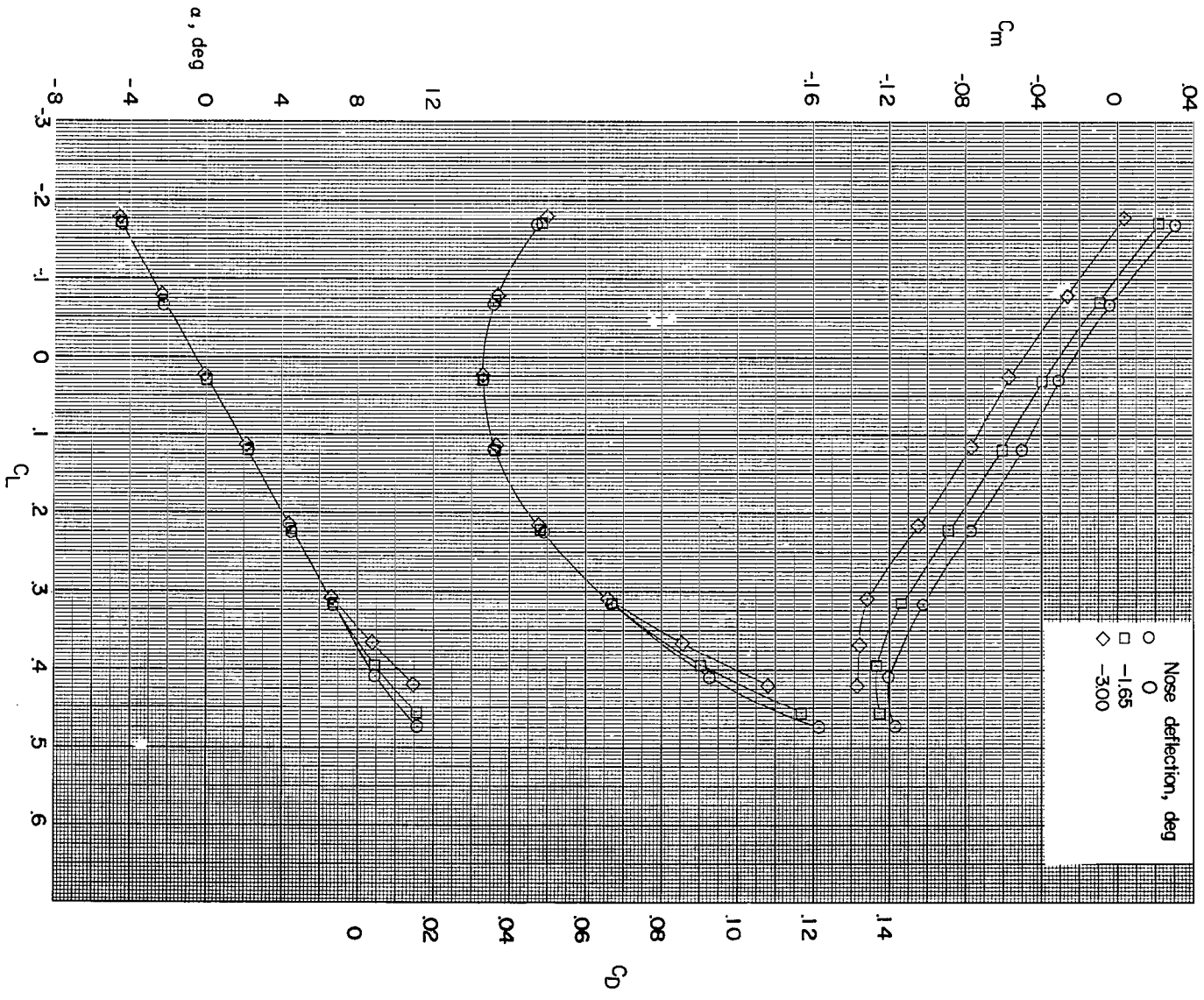


Figure 5.- Effects of nose droop on the aerodynamic characteristics in pitch.  $\delta_{eL} = \delta_{eR} = 0^\circ$ .

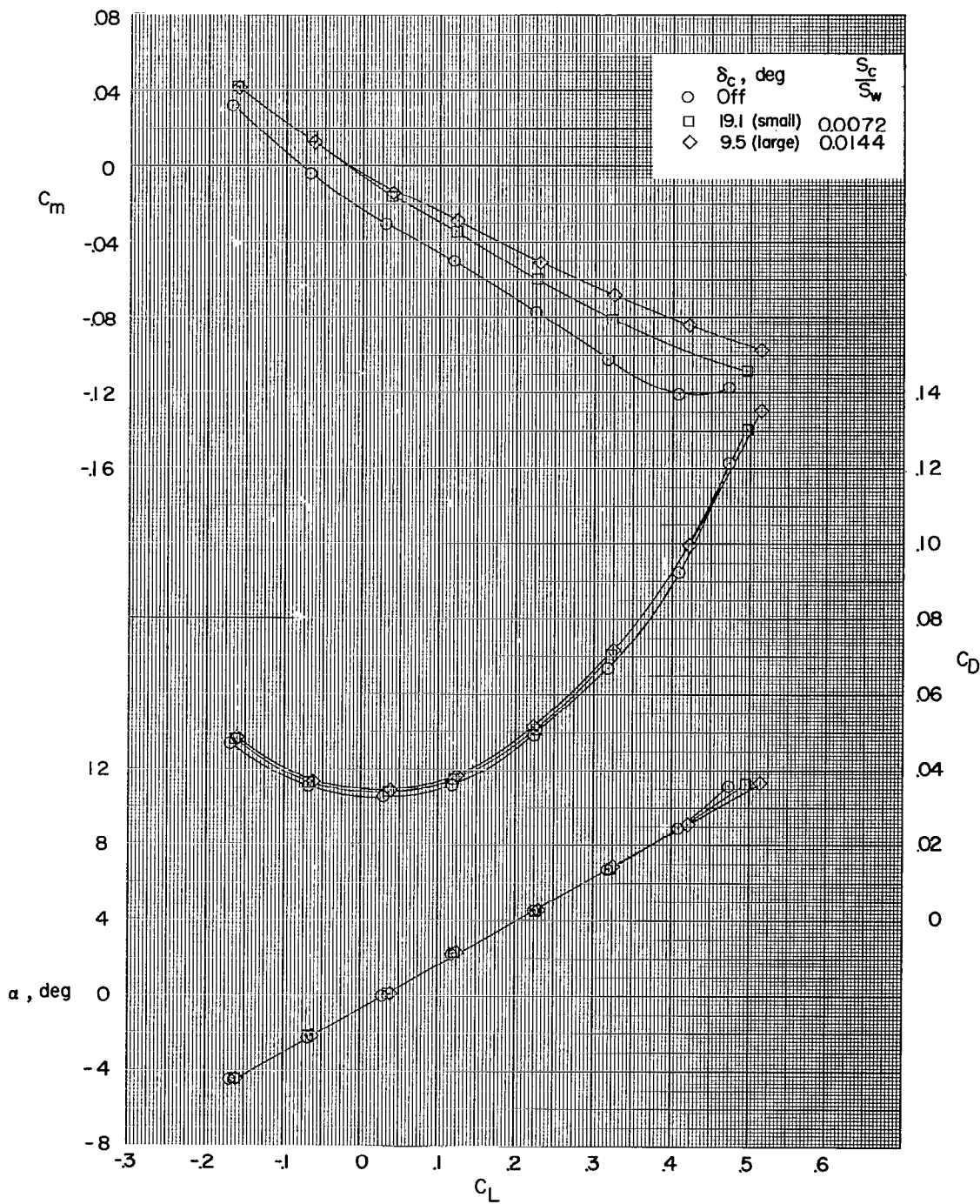


Figure 6.- Effects of canards on the aerodynamic characteristics in pitch.  
 $\delta_{eL} = \delta_{eR} = 0^\circ$ .

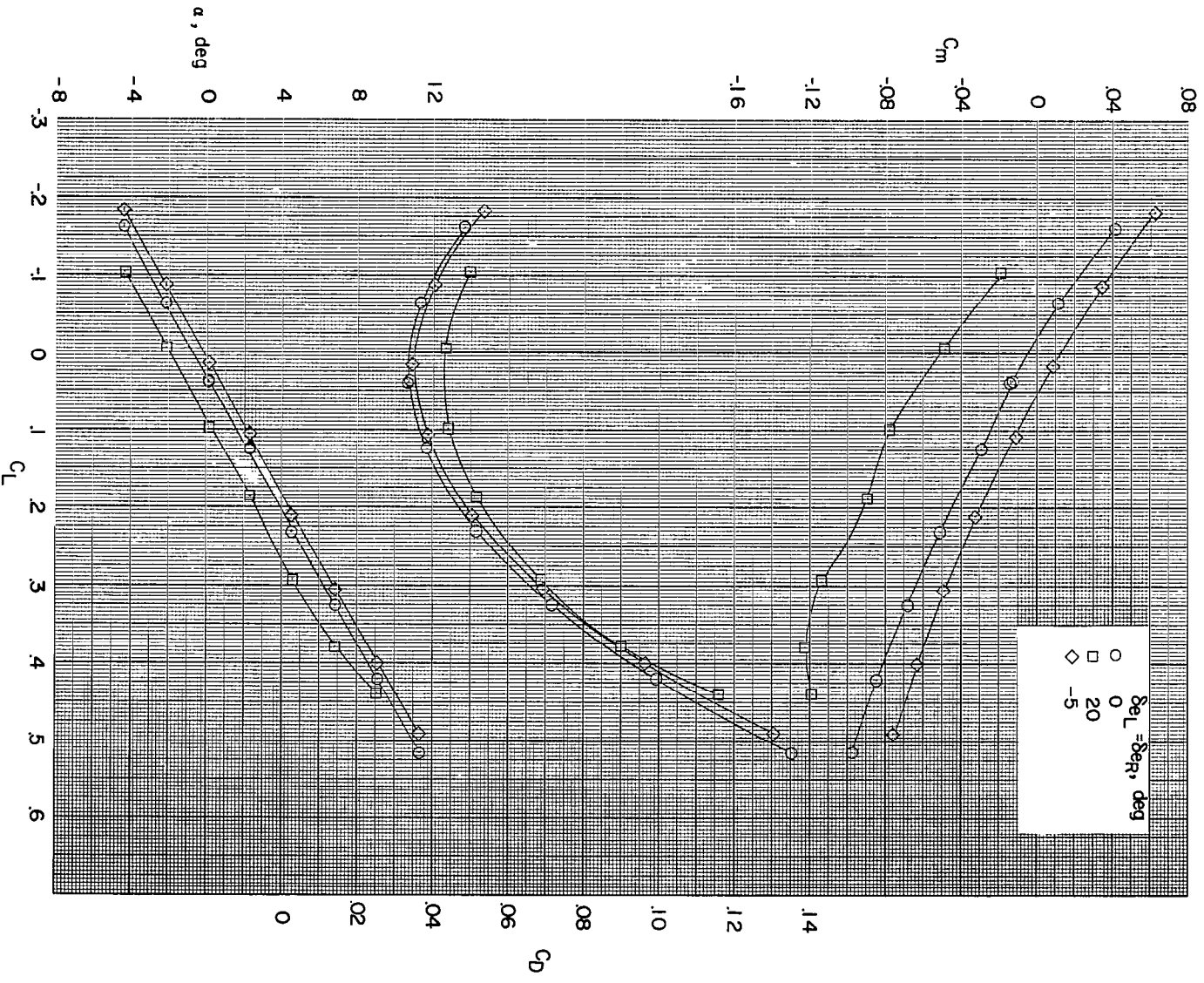


Figure 7.- Effect of eivon deflection on the aerodynamic characteristics in pitch. Large canard,  $\delta_c = 9.5^\circ$ .

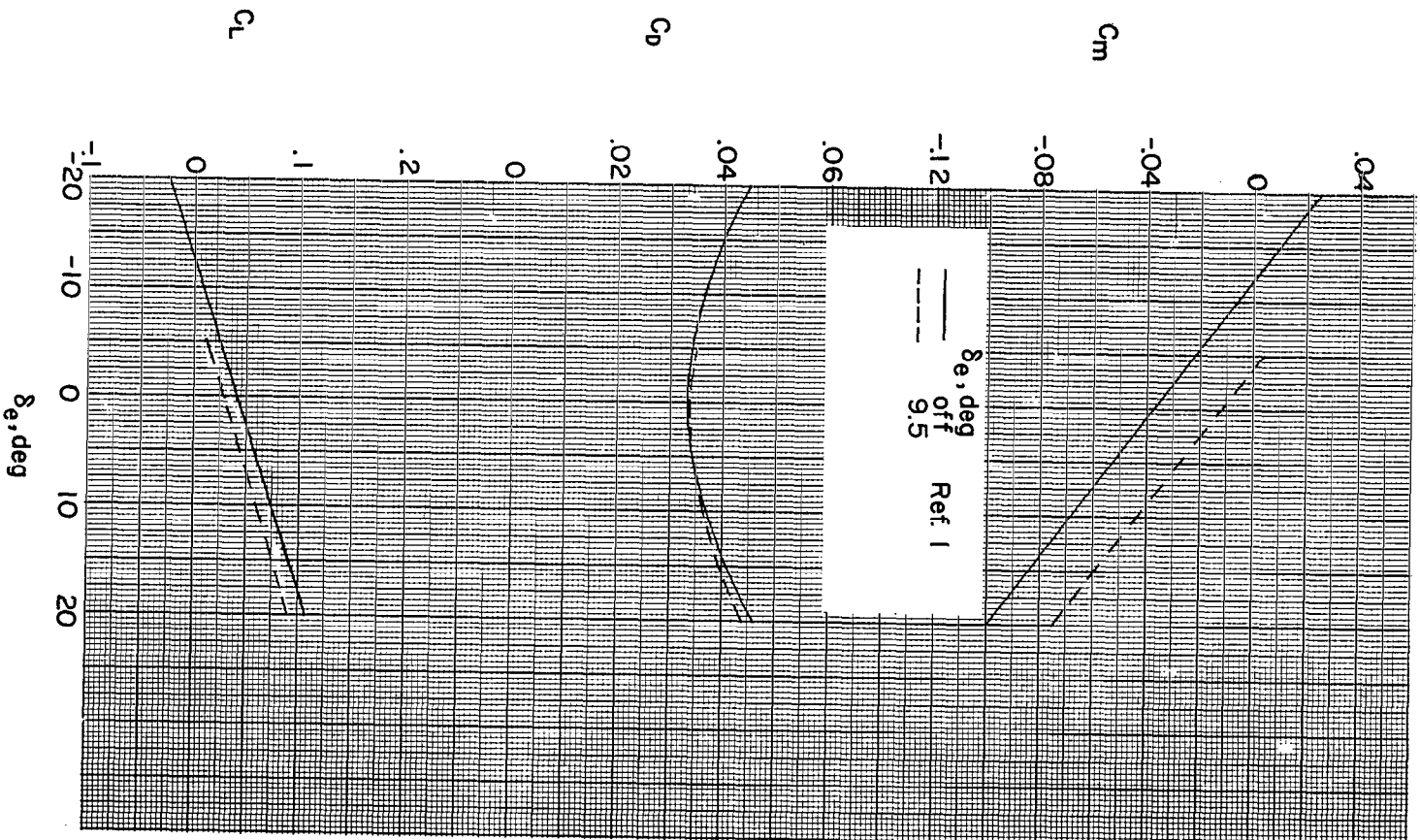
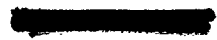


Figure 8.- Effect of the large canard,  $\delta_c = 9.5^\circ$ , on the variation of lift, drag, and pitching-moment coefficients with elevon deflection,  $\alpha = 0^\circ$ .



$\delta_e$ , deg  
 — off Ref. 1  
 - - - 9.5

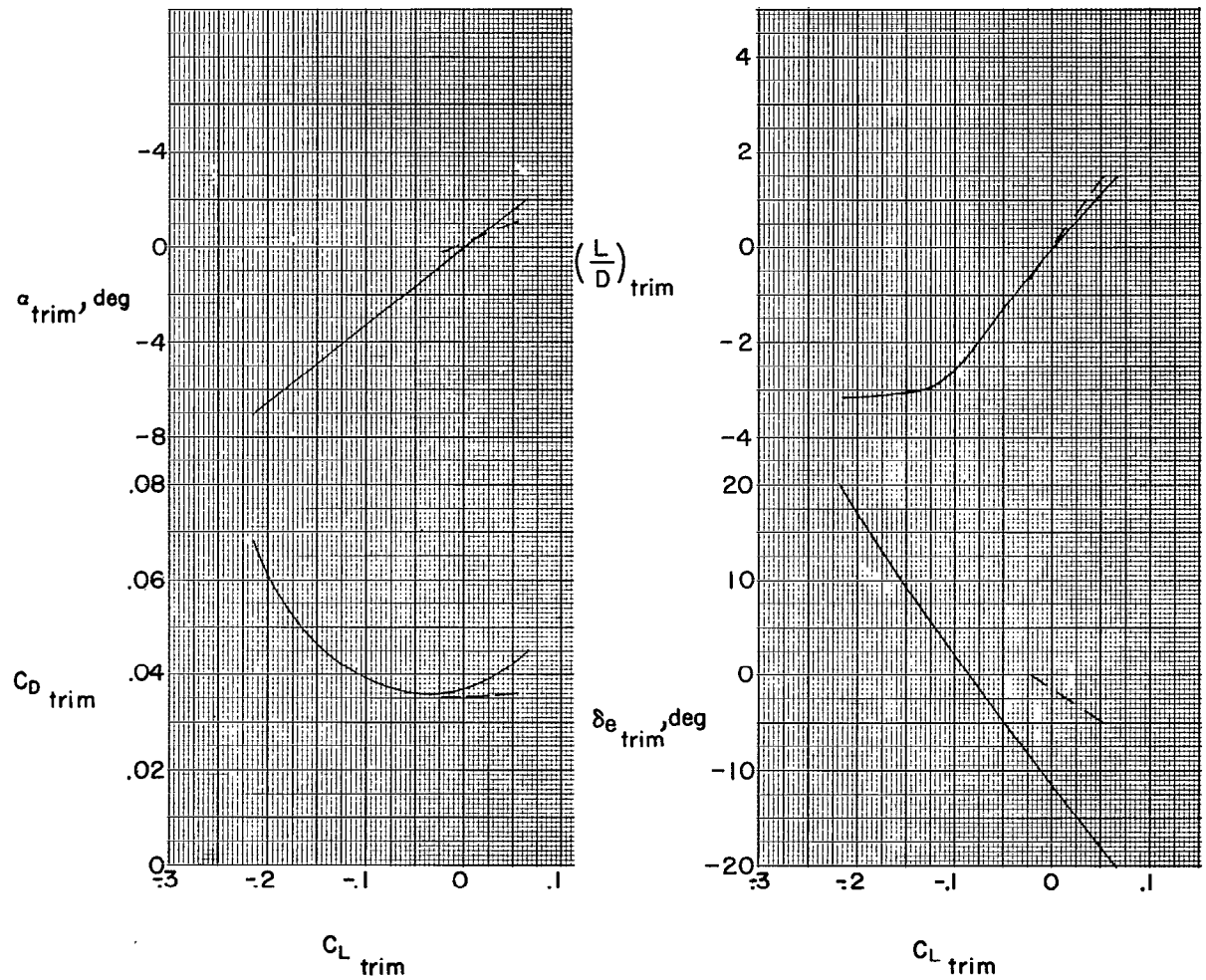


Figure 9.- Effect of the large canard,  $\delta_c = 9.5^\circ$ , on the longitudinal trim characteristics.



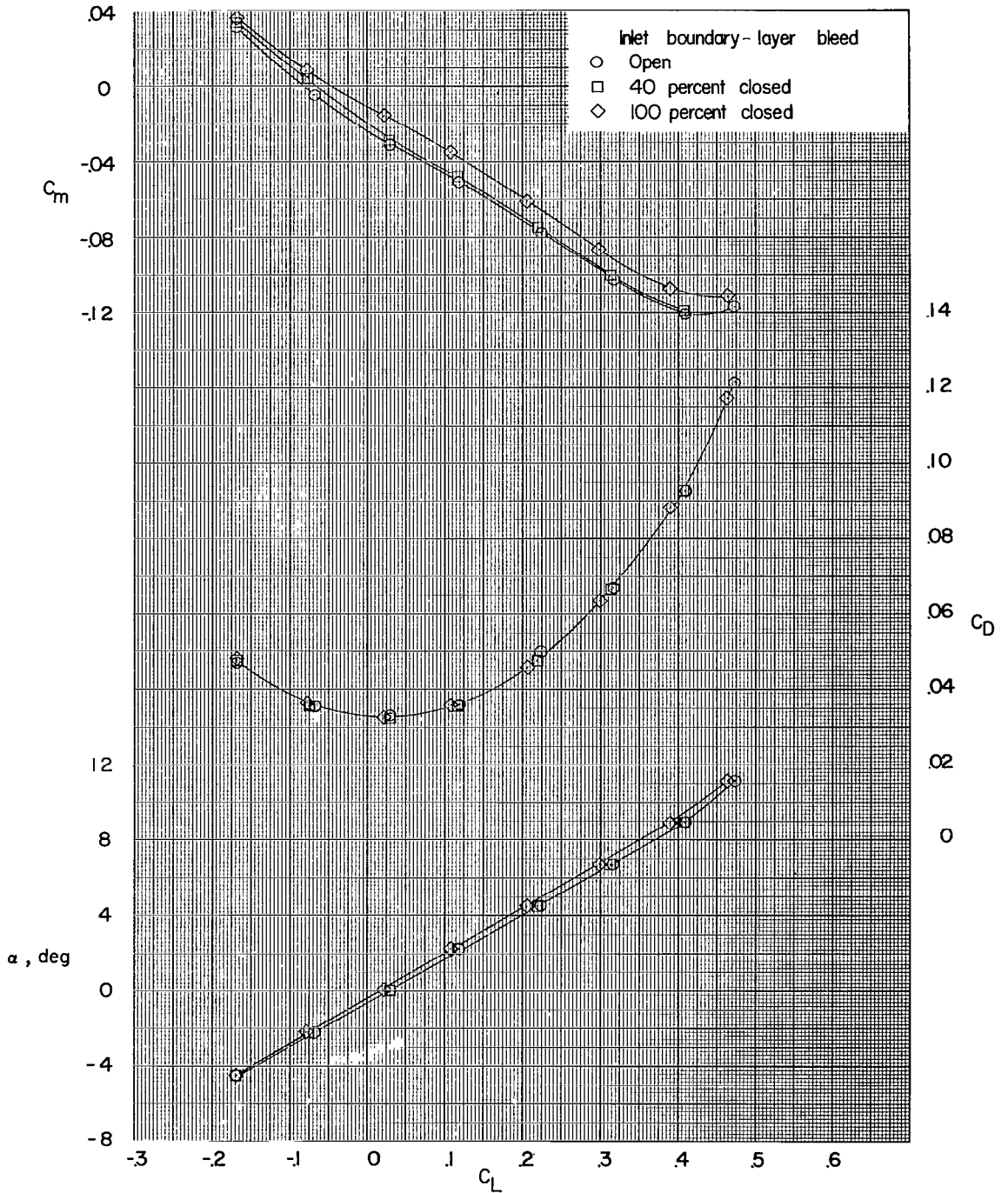


Figure 10.- Effect of varying the amount of boundary-layer bleed closure on the aerodynamic characteristics in pitch.  $\delta_{eL} = \delta_{eR} = 0^\circ$ ; open inlet.

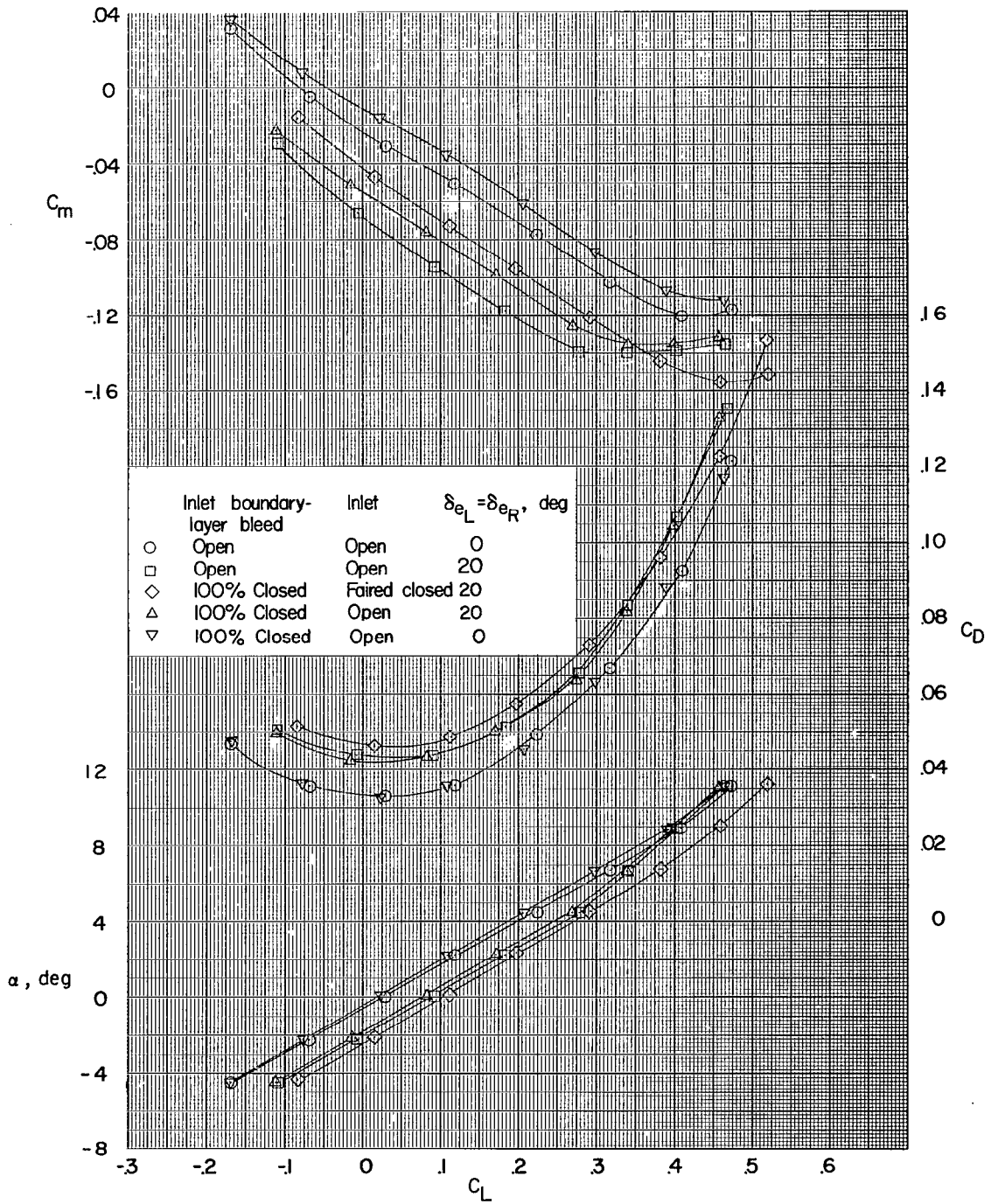


Figure 11.- Effects on the aerodynamic characteristics in pitch of various combinations of boundary-layer closure and open and faired closed inlet for two elevon deflections.

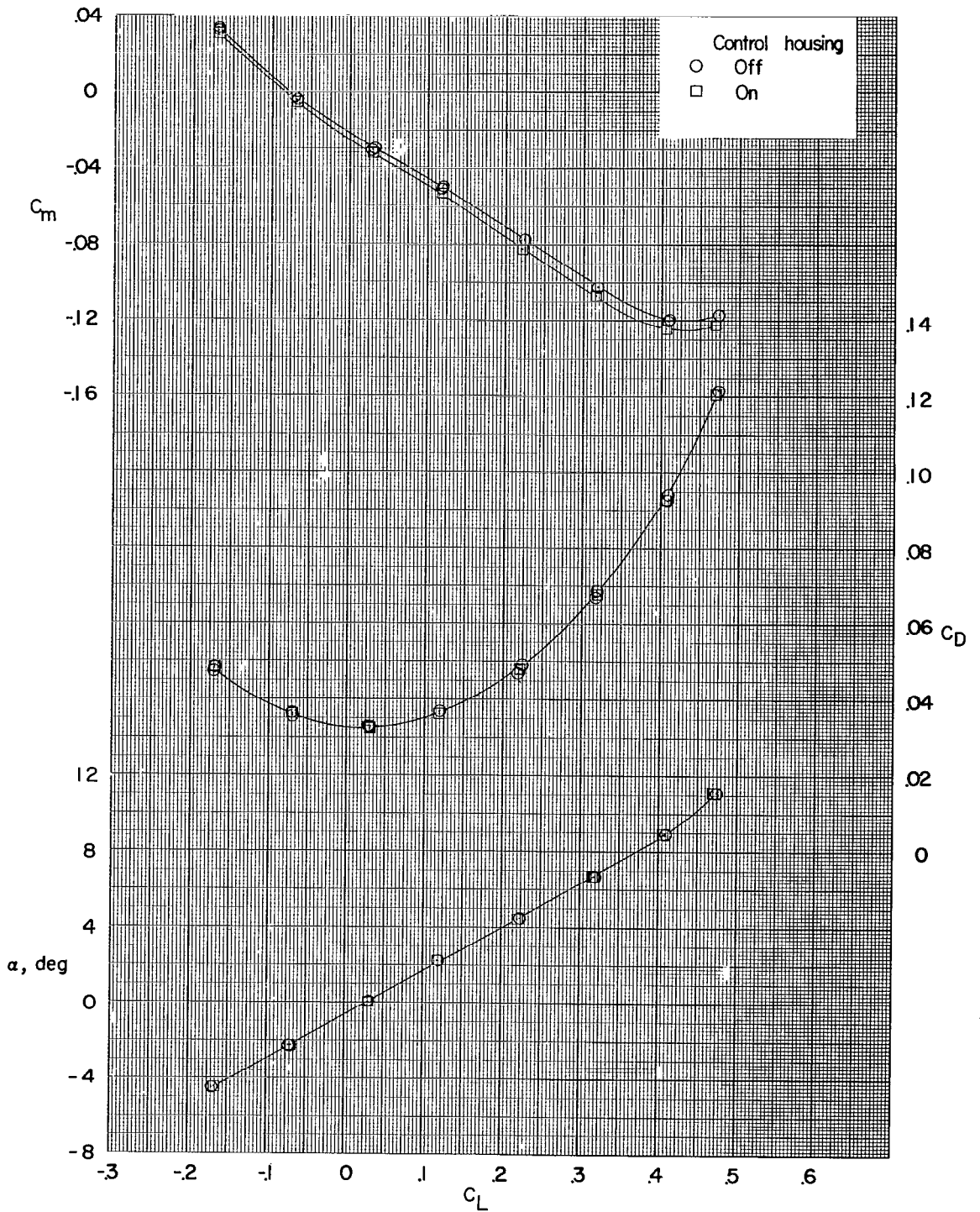


Figure 12.- Effect of control housing on the aerodynamic characteristics in pitch.  $\delta_{eL} = \delta_{eR} = 0^\circ$ .

NASA Technical Library



3 1176 01438 6479

**CONFIDENTIAL**